

# High-speed optical time-division-multiplexed/WDM networks and their network elements based on regenerative all-optical ultrafast wavelength converters

Lavanya Rau, Suresh Rangarajan, Wei Wang, Hsu-Feng Chou, Henrik N. Poulsen, John Bowers, and Daniel J. Blumenthal

*Department of Electrical and Computer Engineering, University of California at Santa Barbara, Santa Barbara, California 93106*

*lavanya@ece.ucsb.edu*

RECEIVED 13 JANUARY 2004; ACCEPTED 15 JANUARY 2004; PUBLISHED 4 FEBRUARY 2004

We describe an optical time-division-multiplexed (OTDM)/WDM network architecture that integrates high-speed optical time-division multiplexing at speeds of 40 Gbit/s and higher with lower-bit-rate WDM channels. An ultrafast wavelength converter is used as a regenerative multifunction building block for OTDM multiplexing, WDM-to-OTDM and OTDM-to-WDM transmultiplexing, OTDM/WDM multicasting, OTDM all-optical label read-write, and all-optical time-channel add-drop multiplexing. Subsystem design and underlying component technologies are described in detail. New results and performance measurements are shown at 40 and at 80 Gbit/s. © 2004 Optical Society of America

*OCIS codes:* 060.4510, 060.4250.

## 1. Introduction

As the increased end-user bandwidth demand drives the need for higher-capacity access networks, there will be a commensurate increase in metropolitan/wide-area (interoffice) and eventually long-haul capacities. Hence it is expected that applications for transmission speeds at 40 Gbit/s and higher will emerge. These higher-speed networks may use optical-time-division-multiplexed (OTDM) approaches to support the assembly and transmission of bit streams in excess of 40 Gbit/s. The handling of bit streams at these speeds at the transmission and network levels as well as interaction with lower-bit-rate access streams is critical for network realization, functionality, and scalability. Hybrid WDM/OTDM networks have been proposed to move data between WDM and OTDM networks, and various subsystems have been demonstrated at 40 Gbit/s including WDM-to-OTDM and OTDM-to-WDM translators, OTDM transmitters, and OTDM add-drop multiplexers. However, the underlying technologies in these systems do not scale beyond 40 Gbit/s and have not addressed other critical functions such as OTDM multicasting, optical labeling, and packet operation.

In this paper we describe an OTDM/WDM network architecture and design and demonstrate its constituent network elements on the basis of a regenerative nonlinear fiber wavelength converter (WC) building block. The underlying technologies used to implement a suite of network functions are described and experimentally demonstrated including WDM-to-OTDM and OTDM-to-WDM transmultiplexers, OTDM add-drop multiplexing, and OTDM multicasting. The ultrafast nonlinear fiber wavelength converter is shown to implement these functions as well as act as a regenerative element at OTDM data rates.

## 2. OTDM/WDM Network Architecture

OTDM/WDM networks that bridge high-bit-rate channels in the core network to lower-bit-rate WDM channels in metro and access networks have been proposed [1–3]. In this paper we focus on the architecture shown in Fig. 1. Multiple low-bit-rate WDM channels are optically multiplexed into a single high-bit-rate channel. The routing within the core is accomplished by either wavelength conversion of the entire high-speed stream or by optical time add-drop of subrate channels within the stream. In addition, the high-speed channels may be optically multicast from one-to-multiple wavelengths. At the egress of the core network the high-bit-rate channel is demultiplexed back to low-bit-rate WDM channels. The network elements and functions that we demonstrate are synchronous in nature, and we assume bit-level synchronization.

Electronic and optoelectronic components that operate at 40 Gbit/s are commercially available for transponder and transmission link implementation. However, more-complex subsystems capable of operating at 40 Gbit/s with the potential to scale to 100 Gbit/s and higher are difficult to realize with today's electronic technologies. This is especially true with switching, multicasting, and add-drop subsystems. All-optical techniques may be exploited to realize these higher-functionality subsystems as well as offer other advantages related to power consumption, performance, and potentially cost. The advantages of performing such functions in the optical domain are scalability to higher bit rates and larger WDM channel count, reduced power dissipation dependence on bit rate, and potentially lower cost at high bit rates.

To implement the OTDM/WDM network architecture shown in Fig. 1, key optical network functions are required. These network functions and the underlying technologies used to implement them are summarized in Table 1. These elements provide the basic level of functionality, connectivity, and scalability required for the OTDM/WDM network. The all-optical fiber wavelength converter is a critical technology because it is used to realize each function and is 2R regenerative at the OTDM bit rates. A key function related to ultra-high-speed transmission that is not covered in this paper is chromatic dispersion compensation, since it has been described in great detail in the literature [4, 5].

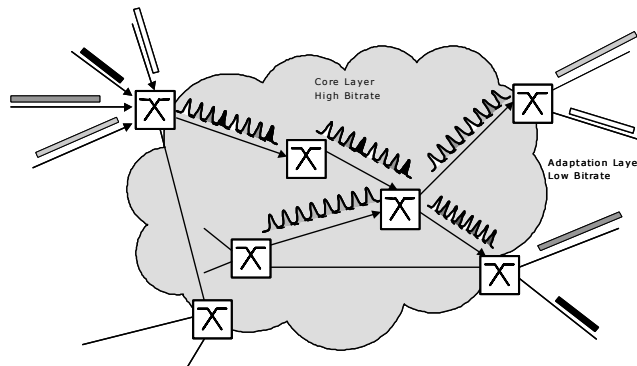


Fig. 1. All-optical OTDM/WDM network architecture.

## 3. Underlying Technologies

### 3.A. All-Optical Fiber Cross-Phase Modulation Wavelength Converter

The ultrafast wavelength converter, used in each network function, is based on cross-phase modulation (XPM) in optical fiber [6]. The converter operates over a wide range of wave-

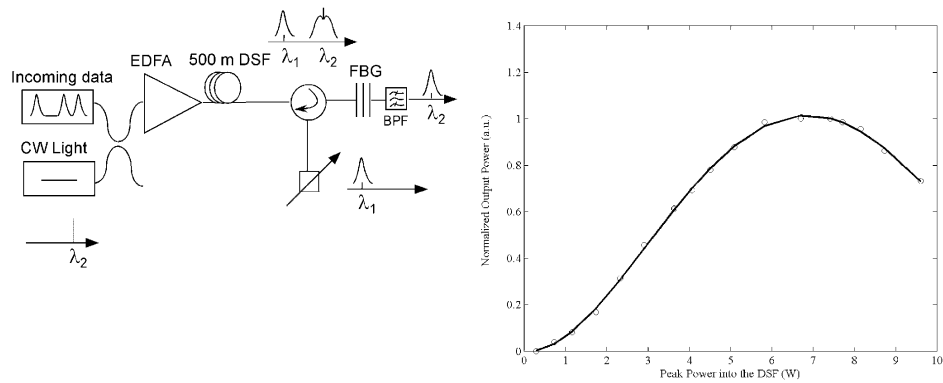


Fig. 2. Schematic of the nonlinear fiber WC with lumped gain.

**Table 1. Optical Network Functions and Underlying Component Technologies**

		Network Functions							
		OTDM Multiplexer/Demultiplexer	WDM to OTDM Trans-Multiplexer	OTDM Wave-length Converter	OTDM Regene-rator	OTDM Add/Drop Multi-plexer	OTDM Multi-casting	OTDM Label Read/ Erase/ Write	OTDM to WDM Trans-Multi-plexer
Underlying Technologies	All-optical fiber XPM wavelength converter	*	*	*	*	*	*	*	*
	Electro-absorption modulator	*	*					*	*
	WDM laser array/tunable laser		*	*		*	*	*	*
	OTDM pulse sources	*	*			*			

lengths (C-band at minimum) and is capable of functioning at data rates from 40 Gbit/s to greater than 100 Gbit/s. The converter is also 2R digitally regenerative and is bit-rate transparent. We describe the design and operation of two versions of this converter, a lumped gain WC based on a front-end erbium-doped fiber amplifier (EDFA) and a distributed gain WC based on Raman amplification in the XPM fiber [7]. Both versions of this converter have been shown to operate at 80 Gbit/s [8, 9].

The lumped gain fiber XPM WC is illustrated in Fig. 2. Its principle of operation is based on XPM in optical fiber followed by optical spectral filtering to convert frequency modulation to amplitude modulation. At the input, an intensity modulated return-to-zero (RZ) data stream at wavelength  $\lambda_1$  is combined with a locally generated continuous wave (CW) optical signal at wavelength  $\lambda_2$ . The incoming data stream at  $\lambda_1$  modulates double sidebands onto  $\lambda_2$  through XPM. The optical carrier and one of the optically generated sidebands are then suppressed by use of optical filtering, and the output consists of an intensity modulated single sideband RZ data stream at  $\lambda_2$ . The optical filtering is performed with a two-stage filter. The first stage is a fiber Bragg grating (FBG) optical filter used to suppress the carrier at  $\lambda_2$  and reject the signal at  $\lambda_1$ . The second-stage bandpass filter (BPF) is used to extract one single sideband. The FBG improves the extinction ratio of

the converted signal through carrier suppression, whereas the second-stage BPF bandwidth is chosen to further improve the extinction ratio and pulse shape of the converted signal. Fiber XPM wavelength conversion has the potential to scale to very high bit rates (>100 Gbit/s) because of the femtosecond nonlinear response. The inset in Fig. 2 shows the WC transfer function (input power versus output power). The 2R regenerative nature of the WC results from the nonlinear shape of the input–output power transfer function. The data noise (amplitude fluctuation) at the one and zero levels is reduced when the WC is operated between the top and the bottom of the nonlinear transfer function.

The distributed Raman gain WC is shown in Fig. 3. The principle of operation is similar to the lumped gain configuration with Raman amplification used in combination with the input EDFA. The advantage of using distributed gain over lumped gain is the ability to optimize the optical signal-to-noise ratio (OSNR) and extinction ratio of fiber XPM. By use of highly nonlinear dispersion-shifted fiber (HNLDSE) the fiber length and input peak power can be reduced. The conversion bandwidth can also be increased to almost the entire C band at 80 Gbit/s [9]. Compared with lumped amplification, this scheme significantly improves the signal-spontaneous beat noise performance at the receiver by amplifying the signal channels while they are in the transmission fiber. It also reduces the amount of cross talk from the pump light by means of reducing the amount of self-phase-modulation (SPM) of the pump light while maintaining the same conversion efficiency.

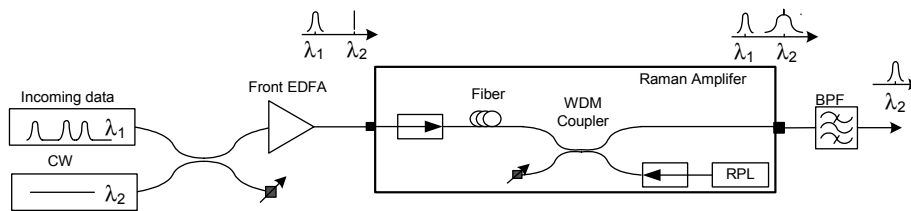


Fig. 3. Schematic of the nonlinear fiber WC with distributed gain.

### 3.B. Electroabsorption Modulator

Electroabsorption modulators (EAMs) are also used in multiple network functions including the OTDM mux–demux, transmultiplexers, optical label read–erase–write, and OTDM add–drop multiplexers. The high bandwidth and modulation efficiency of these devices makes them very attractive as 10–40 Gbit/s data modulators, and their fast response time makes them capable of demultiplexing directly 160 Gbit/s down to 10 Gbit/s [10]. The EAMs used in these experiments were fabricated at the University of California at Santa Barbara [11] and use traveling-wave electrodes that extend the active device length without limiting the speed, because of the RC time constant. The longer device length improves the saturation power as well as the modulation efficiency, both critical factors in device performance.

In OTDM systems, the EAM is used as an ultrafast optical gate that must provide switching windows of the order of picoseconds with on–off contrast ratios in excess of 15 dB. EAMs are typically driven at the electrical input with a sinusoidal signal at the base rate of the OTDM data stream. For example, an 80-Gbit/s OTDM data signal can be optically demultiplexed to 10 Gbit/s by use of a single EAM; this enables the use of simple 10-Gbit/s receiver technology. To enhance the single-frequency performance of EAM, a standing-wave design can be used to increase the electric field amplitude inside the device. The electrical standing-wave pattern is formed along the traveling-wave electrodes

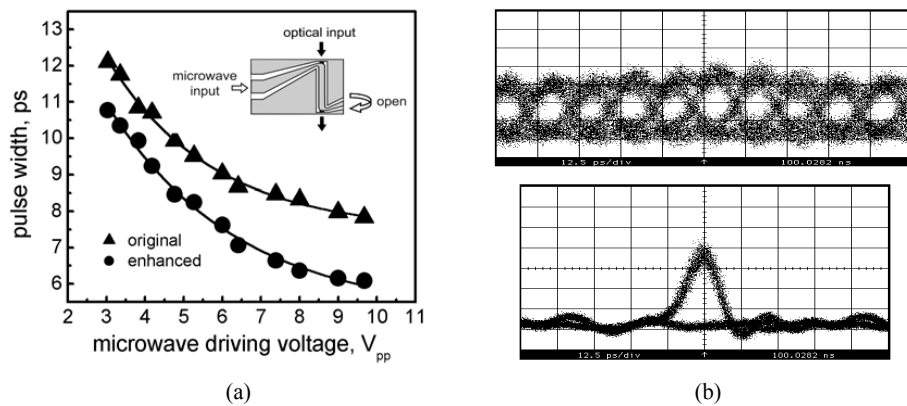


Fig. 4. (a) Input–output transfer function for a traveling- or standing-wave electroabsorption modulator (EAM). (b) 80-Gbit/s data stream demultiplexed from to a 10-Gbit/s channel with an EAM.

as shown in Fig. 4(a). This design was applied to generate optical switching windows as short as 3.4 ps [12] and used to reduce the microwave driving voltage required for 80–10-Gbit/s OTDM demultiplexing [13]. An example of an 80-Gbit/s data stream optically demultiplexed to 10 Gbit/s is shown in Fig. 4(b).

### 3.C. OTDM Pulse Source

A basic element needed for high-speed OTDM is a short-pulse source. To achieve transmission at 40 Gbit/s and greater, it is necessary to generate pulses with  $< 10$  ps rms widths and  $< 2$  ps jitter, and an extinction ratio (ER)  $> 28$  dB is required for lower interferometric cross talk [14].

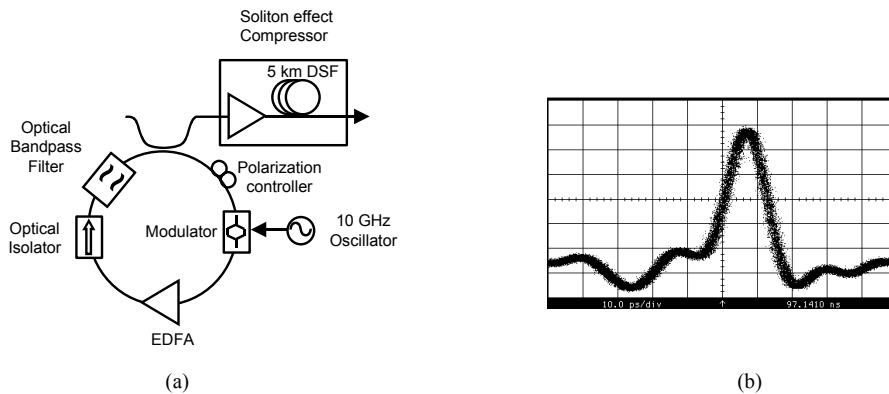


Fig. 5. Setup (a) and oscilloscope trace (b) of the mode-locked fiber ring laser.

The source optical signal-to-noise ratio (OSNR), defined by measuring the signal power relative to the total optical noise within a 0.1 nm optical bandwidth, of  $> 25$  dB is required for achieving a bit-error-rate (BER) better than  $10^{-12}$ . It is possible to generate these pulses with EAMs, gain-switched lasers, and ring lasers. Actively mode-locked fiber ring lasers can generate short transform-limited pulses with low jitter at repetition rates of 40 GHz

[15]. In the demonstrations of the network elements described in this paper, we employ an actively mode-locked fiber ring laser capable of generating 5–8-ps pulses with supermode suppression  $> 70$  dB and measured jitter less than 200 fs, which can also be used to generate a burst of pulses [16]. For data rates higher than 40 Gbit/s we use a pulse compressor to shorten the pulses to 2–3 ps. Figure 5 shows the experimental setup and the oscilloscope trace of the ring laser.

The fiber ring laser can be made compact but still occupies the footprint of a module, because of the length of fiber required. Alternate pulse-generation techniques using gain-switched laser diodes and EAMs have been demonstrated [12, 17]. Recently optical pulses at 160 GHz were generated by active mode locking of a semiconductor laser [18].

#### 4. Network Elements and Experimental Demonstrations

##### 4.A. All-Optical WDM-to-OTDM Multiplexer

The WDM-to-OTDM multiplexer function enables  $W$  wavelengths, each non-return-to-zero (NRZ) modulated at  $B$  Gbit/s, to be multiplexed to an RZ-modulated OTDM single-wavelength data stream at  $W \times B$  Gbit/s. This element directly converts an array of WDM transmitters to an OTDM channel or acts as a bridge between WDM and OTDM networks without requiring passage of the signals through electronics. The WDM-to-OTDM multiplexer operation from  $4 \times 10$  Gbit/s NRZ to 40 Gbit/s RZ using the nonlinear fiber XPM converter was demonstrated in Ref. [19]. Amplitude fluctuations that result from passive multiplexing are reduced by this technique. Other approaches of WDM-to-OTDM transmultiplexing using a nonlinear optical loop mirror [20], EAM [21], and four-wave mixing in a semiconductor optical amplifier (SOA) [22] have also been proposed and demonstrated.

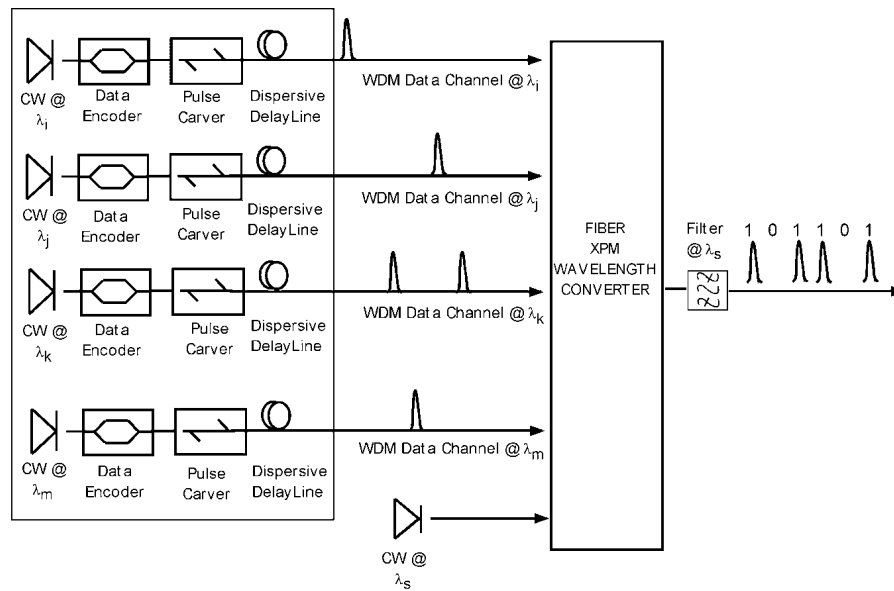


Fig. 6. WDM-to-OTDM all-optical multiplexing.

The basic principle of operation is illustrated in Fig. 6. A WDM laser array is used to generate  $W$  wavelengths, each transmitting at NRZ bit-rate  $B$  Gbit/s. The outputs are converted from NRZ-to-RZ pulses using the EAM as a pulse carver (a single EAM may

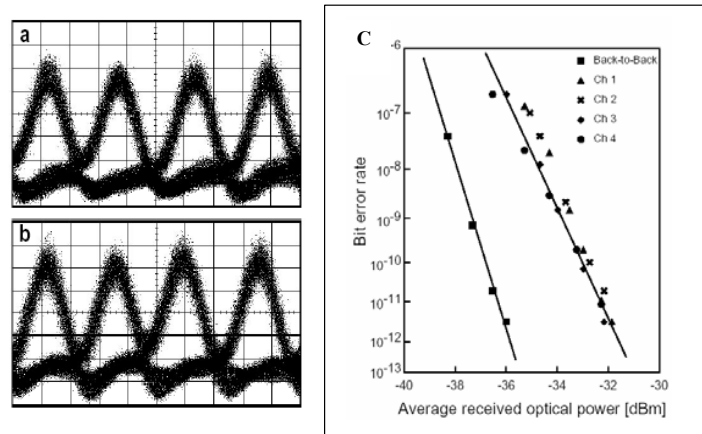


Fig. 7. Eye patterns of the  $4 \times 10$  Gbit/s WDM channels (a) before wavelength conversion, (b) the output 40-Gbit/s OTDM data after wavelength conversion, and (c) measured BER for input 10-Gbit/s channel (BtB) and the four time channels at the output 40-Gbit/s OTDM data.

also be used to carve all WDM source simultaneously). A dispersive delay line is then used to stagger the pulses in  $1/(B \times W)$ -ps increments. The  $W$  staggered data-modulated pulse trains and local CW source (at a wavelength different from the input wavelengths) are copropagated through a XPM fiber WC.

The cumulative set of eye patterns for the time-staggered four individual 10-Gbit/s WDM channels after the EAM and the dispersion delay line are shown in Fig. 7(a). Figure 7(b) shows the single 40-Gbit/s OTDM stream after the WC. BER measurements were performed on the output by demultiplexing of the data into four 10-Gbit/s channels. BER measurements were performed on each of the four OTDM channels by demultiplexing of the 40-Gbit/s data. A 3-dB receiver power penalty at a BER of  $10^{-9}$  was observed between one of the original 10-Gbit/s NRZ channels and all the demultiplexed OTDM channels. The penalty is primarily the result of cross talk between the WDM channels in the first EAM in the NRZ-to-RZ conversion process, and also partly the result of the high loss in the EAM, which decreases the signal-to-noise ratio (SNR) after the EDFA.

#### 4.B. All-Optical OTDM-to-WDM Demultiplexer

Simultaneously demultiplexing OTDM to WDM is possible with the fiber-based XPM WC and was demonstrated in Ref. [23]. This technique has the potential to operate at high bit rates over a wide wavelength range. Other approaches to multichannel demultiplexing include InP Mach-Zehnder interferometer converters [24], four-wave mixing (FWM) in semiconductor optical amplifiers [26], and FWM via super continuum light-source generation in a highly nonlinear fiber [25].

The fiber XPM simultaneous demultiplexer operates as illustrated in Fig. 8. An  $N$ -channel RZ OTDM data stream at wavelength  $\lambda_i$  and bit rate  $B$  Gbit/s is demultiplexed into lower-bit-rate channels, each on a different output wavelength  $\lambda_{1-N}$ . The  $N$  WDM local control pulses are generated by a set of CW fixed-frequency lasers that are combined and pulse modulated by a single EAM at the repetition rate  $B/N$ . The EAM switching window is slightly larger than the input OTDM pulses. At the output of the EAM,  $N$  temporally overlapping WDM control pulses with repetition rate  $B/N$  are found.

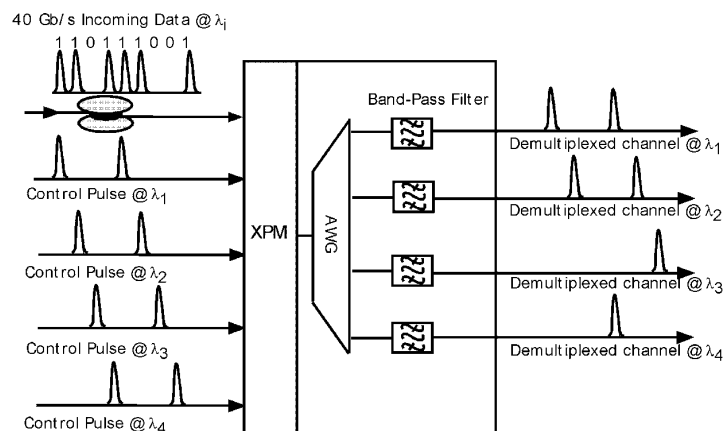


Fig. 8. Principle of simultaneous OTDM-to-WDM demultiplexing with a fiber XPM WC.

A dispersive delay line (optical fiber) is used to separate these pulses into  $N$  temporally discrete clock channels each  $(1/B)$  s apart. The EAM switching window is synchronized with the input OTDM data by use of a clock recovery circuit in order to align the WDM control pulses with the OTDM input. Both WDM control pulses and OTDM pulses are copropagated in the dispersion-shifted fiber (DSF) such that every WDM control pulse overlaps with one of the time channels from the incoming data stream. The incoming intensity-modulated OTDM signal generates double sidebands on each WDM channel (via XPM) corresponding to the data in the synchronized time slot. One of these sidebands is filtered to convert phase modulation to amplitude modulation. A WDM filter, such as an arrayed waveguide (AWG) of appropriate filter bandwidth, can be used for simultaneously filtering and separating the sidebands for all WDM channels. BPFs at the output of the AWG help in further improving the extinction ratio and the pulse shape of the demultiplexed signals. Further experimental details are reported in Ref. [23].

The measured eye diagrams for the input 40-Gbit/s OTDM signal and four 10-Gbit/s demultiplexed channels are shown in Fig. 9. The measured demultiplexed pulses were broader than the input pulses because of the narrow-bandwidth optical filter that is used to obtain the demultiplexed channel. The measured BER curves for the original 10-Gbit/s data filtered with a 0.2-nm BPF (back-to-back) and the four demultiplexed 10 Gbit/s channels are shown in Fig. 10. There is a maximum penalty of 1 dB (at BER  $10^{-9}$ ) observed between the back-to-back and one of the four demultiplexed channels.

The power penalty can be attributed to the channel interference that results from passive multiplexing to generate OTDM data, the high loss in the EAM, which decreases the SNR of the generated control pulses after amplification and the process of demultiplexing. Because both the EAM and the WC are polarization sensitive, the polarization dependence of the system is approximately 2–3 dB. Unlike in other schemes, the demultiplexing window in this technique is determined by the pulse width of the incoming data signal, and thus the local clock pulses can be broad; for example, in this demonstration the local clock pulses were as broad as 14.0 ps.

#### 4.C. All-Optical OTDM Add-Drop Multiplexer

The OTDM time-channel add-drop multiplexer is used to extract and inject data directly into the OTDM bearing portion of the network. Various methods of performing OTDM

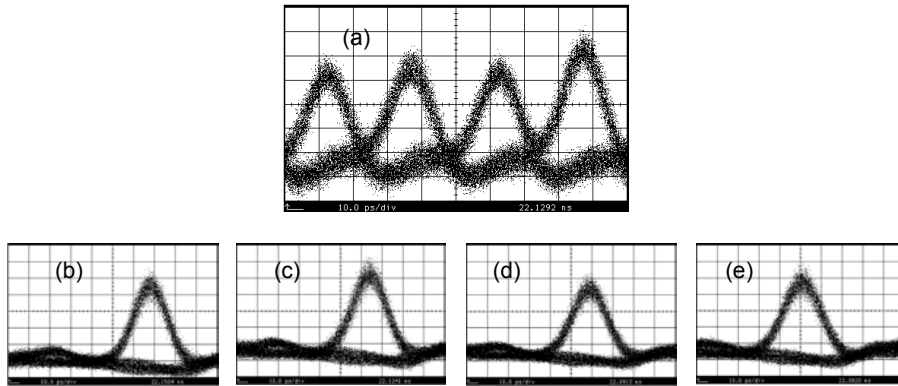


Fig. 9. (a) Input OTDM data at 1554.0 nm and simultaneously demultiplexed channels at (b) 1544.5 nm, (c) 1546.3 nm, (d) 1548.1 nm, and (e) 1549.9 nm.

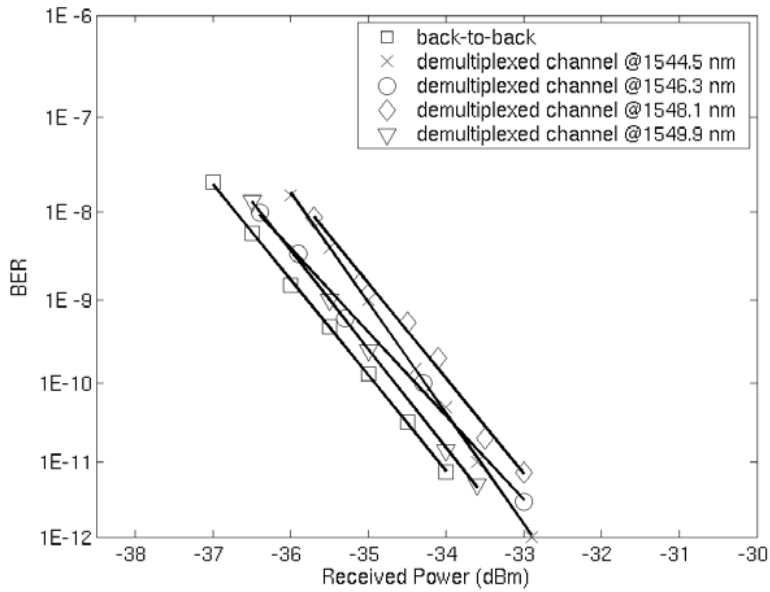


Fig. 10. BER curves for back-to-back and the four simultaneously demultiplexed outputs.

add-drop (OTDM-AD) have been demonstrated to date. All-optical techniques include using an EAM to drop and insert a channel [27] and a monolithic InP Mach-Zehnder interferometer [28]. The fiber XPM converter can also be used to perform this function. Dropping a 10-Gbit/s data channel from an incoming 40-Gbit/s OTDM data signal and inserting a new 10-Gbit/s data channel in its place while performing 2R regeneration on the through-going data was demonstrated in Ref. [29].

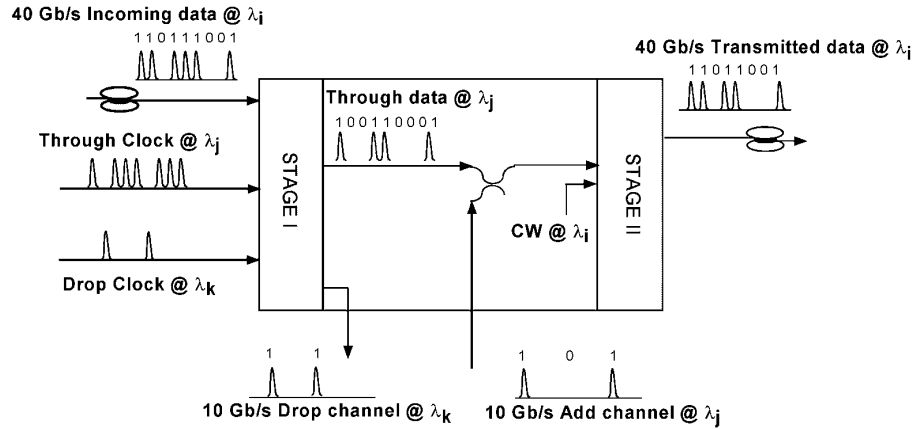


Fig. 11. OTDM add-drop multiplexer.

The OTDM-AD is illustrated in Fig. 11. An incoming OTDM data stream at any wavelength  $\lambda_i$  is input to the first stage of the OTDM-AD. A local 10-GHz drop clock at any wavelength  $\lambda_k$  is synchronized with the channel to be dropped from the incoming signal. A local through clock at an internal wavelength  $\lambda_j$  is synchronized with the remaining channels of the incoming data signal. We obtain the through clock by multiplexing a 10-GHz pulse stream such that there are three pulses that are 25 ps apart and the fourth time slot is empty.

This technique, coupled with a local pulse source with good extinction ratio, yields a good clearing in the empty slot so that a new data channel can be inserted in this empty slot with minimal power penalty. In the first stage of the OTDM-AD the incoming data signal is demultiplexed into the drop channel at  $\lambda_k$  and a through channel at  $\lambda_j$  by wavelength conversion in DSF. At the output of the first stage a new 10-Gbit/s channel at  $\lambda_j$  is added in the empty time slot of the through channel. A second WC is used to convert the multiplexed through channels and the new add channel to the original incoming wavelength  $\lambda_i$ . The second WC is required only if the through signal needs to be at the original incoming wavelength, since self-wavelength conversion is not possible in such a WC.

The results for this implementation are summarized in Figs. 12 and 13. The eye diagrams of the input 40-Gbit/s data stream, the drop channel, the through channels, and the transmitted channels before and after transmission are shown in Fig. 12. The eye diagrams indicate clear open eyes; regenerative capability is also evident from the improvement of extinction ratio improvement and the equalization of the pulse heights before and after the WC.

The 40-Gbit/s transmitted channels were demultiplexed to 10 Gbit/s by use of an EAM. BER measurements were performed on each 10-Gbit/s channel individually, and the resulting BER curves are shown in Fig. 13. The gray dashed curves indicate the BER curves of the transmitted channels after 50 km of DSF. As can be observed from the figure there is

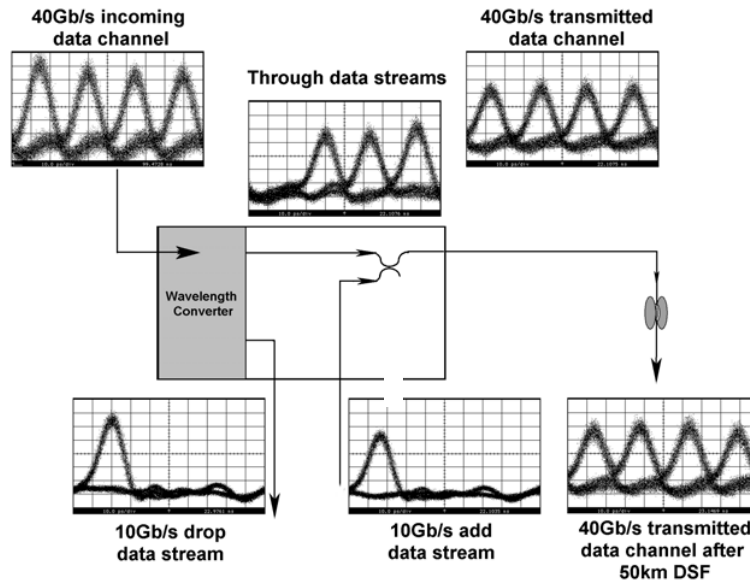


Fig. 12. Eye diagrams for all optical OTDM add-drop multiplexer demonstration.

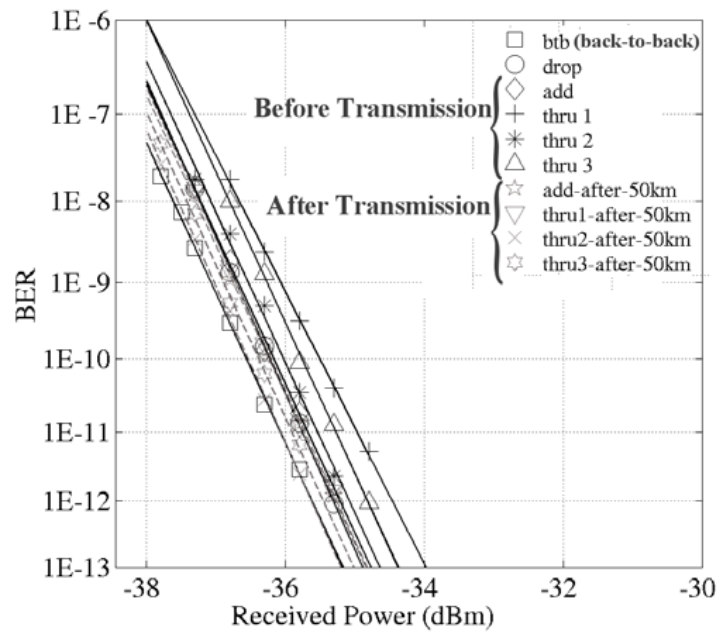


Fig. 13. BER curves for all the channels before and after transmission.

a maximum power penalty of approximately 1 dB between the 10-Gbit/s back-to-back and the worst of the through channels. The reason for this power penalty is that the through clock pulses were not exactly 25 ps apart. It can also be observed from the figure that there is an improvement in the power penalty after transmission; this we believe is due to the compression from being transmitted in the anomalous dispersion region.

#### 4.D. All-Optical OTDM Wavelength Multicasting

The ability to multicast high-speed data with today's electronic techniques can be prohibitively expensive, cumbersome, and power hungry as bit rates climb to 40 Gbit/s and above. All-optical multicasting approaches have the potential to address these issues. We have demonstrated the use of the all-optical WC to multicast at 40 Gbit/s [30].

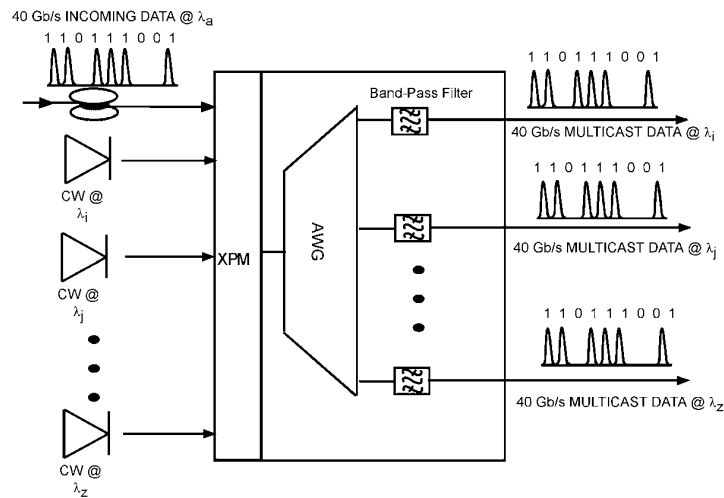


Fig. 14. Optical multicast scheme.

The novelty of this approach is that we do not split the original optical power into multiple copies. The data are replicated simultaneously on multiple wavelengths within a single WC. The broadcast channels can be chosen on a packet-by-packet basis to enable or disable broadcast services to different users. The nonlinear wavelength-conversion process also performs 2R regeneration of the original data signal as seen by an equalization of output RZ pulse levels. The multicast scheme is illustrated in Fig. 14. The incoming signal imposes phase modulation on different CW signals simultaneously by use of XPM in fiber. The phase modulation causes spectral broadening of the CW signals. A WDM filter such as an AWG is used for simultaneously routing and filtering the spectrally broadened phase-modulated channels. The wavelengths of the CW signals are chosen such that they are notched out by the AWG, and the sidebands generated by XPM are routed to different ports of the AWG. A second BPF is used to further improve the extinction ratio and pulse shape of the multicast channels. The results of the wavelength multicast demonstration at 40 Gbit/s are shown in Figs. 15 and 16 below.

Figure 15 shows the receiver sensitivity for all 4 input (back-to-back) channels and the 32 output 10-Gbit/s channels. The receiver sensitivity for the input channels was measured to approximately  $-35.0$  dBm, whereas the receiver sensitivity for the output channels ranged from  $-34.1$  dBm to  $-35.2$  dBm. For each of the eight multicast wavelengths, the demultiplexed 10-Gbit/s OTDM channel with the lowest receiver sensitivity was selected,

and a complete BER plot was obtained. From Fig. 16, it is observed that the maximum power penalty for multicasting with this scheme was 1.5 dB.

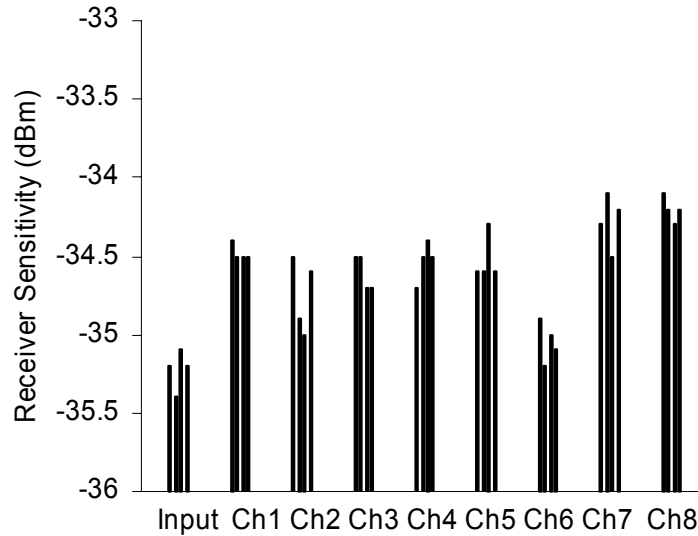


Fig. 15. Measured receiver sensitivity for each of the 32 10-Gbit/s output OTDM channels and the 4 10-Gbit/s OTDM channels.

#### 4.E. Optical Label Read-Write

The capability to monitor and manage data streams and resources is critical in the deployment, management, operation, and reliability of optical networks [31]. Optical labels are carried on data streams and can be attached, read, removed, and replaced without converting the primary to the optical domain. This capability allows network-level information to be carried with data and monitored and manipulated at various points in the network. Optical labels can be used in circuit-switched, burst-switched, or packet-switched networks [32]. Optical labels using optical subcarriers or serial time domain are two approaches that have been demonstrated. Subsystems that allow labels to be inserted and replaced with scaling to high bit rates and providing regenerative functionality are critical to future networks. In this section we describe how the fiber XPM converter can satisfy these requirements.

An example of optical labels for an OTDM packet-switched network is illustrated in Fig. 17. Packets entering the network at an ingress router are encapsulated with a low-bit-rate optical label. The routing hardware within the network is designed to handle packets independent of their bit rate yet be able to process optical labels to make routing decisions. Each optically labeled packet is forwarded to a core optical packet router whose function is to remove the label, read the label, electronically compute a new wavelength and label, attach a new label to the packet, and convert the packet and label to a new optical wavelength. Since the optical labels are at low bit rates, the routing process is fast and low cost. At the network egress router, optical labels are removed and the packet is handed back in the same form it entered the network.

The label-swapping function may be implemented at 40- and 80-Gbit/s rates and higher by use of the fiber XPM WC [8]. This approach has been demonstrated with the configuration in Fig. 18. The label-processing layer is electronic and used to compute the new label

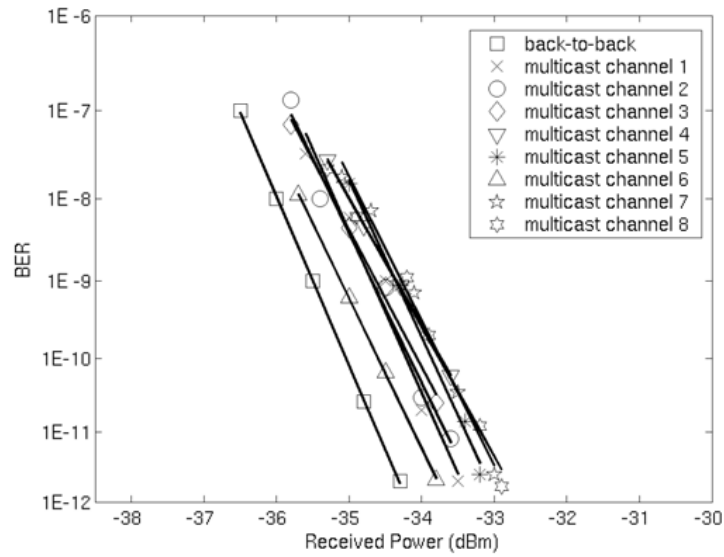


Fig. 16. BER curves for one input channel (back-to-back) and one channel for each of the eight broadcast wavelengths.

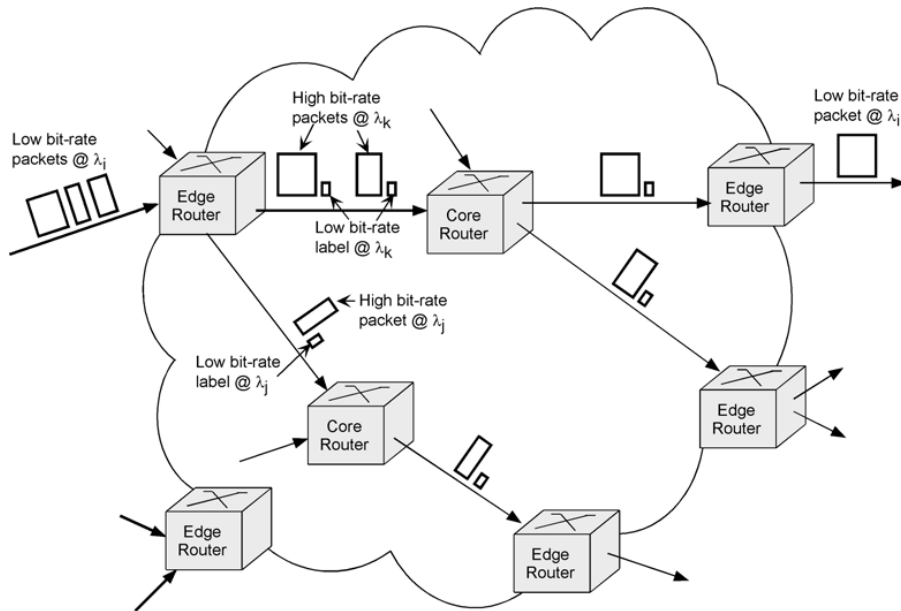


Fig. 17. AOLS system architecture example with ingress, core, and egress routers.

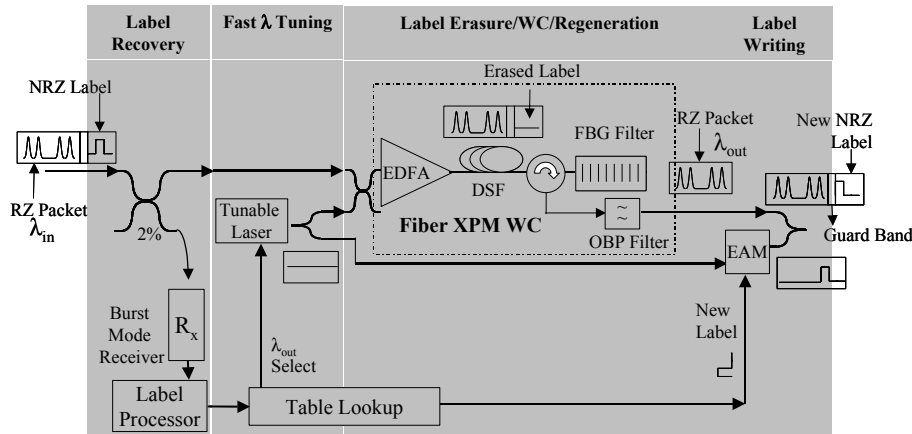


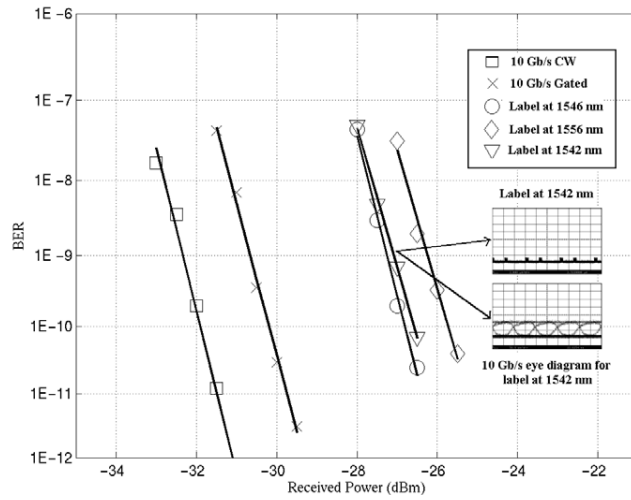
Fig. 18. Implementation of all-optical label eraser-adder.

as well as the outgoing wavelength. Packets are coded using the RZ format and optical labels coded using NRZ format. The fiber XPM converter erases the NRZ label and converts the RZ packet to the new outbound wavelength determined by the NRZ label. While the RZ packet efficiently modulates sidebands through fiber XPM onto the new CW wavelength, the NRZ label is not efficiently converted by XPM and the label is erased. The converted packet with the erased label is passed to the converter output where it is reassembled with the new label, which has been prewritten onto a local laser.

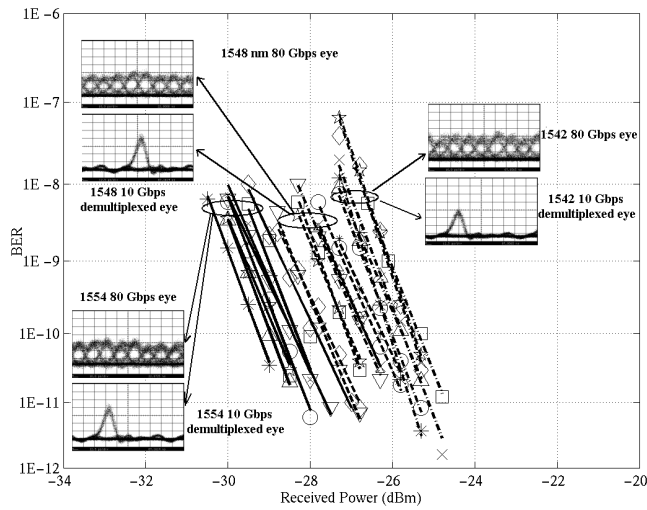
This all-optical label-swapping (AOLS) scheme was implemented for optical packets at 80-Gbit/s converted to two different wavelengths. BER measurements of the wavelength-converted packets after label swapping are shown for each of the 10-Gbit/s demultiplexed channels in Fig. 19(a). The solid curves are the BER curves for the original 1555-nm packet. A power penalty of  $\sim 2$  dB is observed for the 1548-nm wavelength-converted packets, shown by the dashed curves, and a power penalty of  $\sim 3$  dB is observed for the 1542-nm wavelength-converted packets, shown by the dashed-dotted curves. The increase in the power penalty for the 1542-nm packets is due to the increased loss in the EAM. Figure 19(b) shows the BER curves for labels that have been erased and rewritten. A power penalty of  $\sim 4$  dB is incurred at the first hop, and an additional power penalty of 1 dB is incurred at the second hop.

## 5. Conclusions

In this paper we have presented a WDM/OTDM network architecture and key subsystems that are designed and built around a common building block: the ultrafast nonlinear fiber cross-phase modulation (XPM) WC. These subsystems include OTDM multicasting, WDM-to-OTDM and OTDM-to-WDM translation, OTDM add-drop multiplexing, and optical label replacement. The ultrafast WC is demonstrated to operate at 40 and 80 Gbit/s and has the capability to scale to bit rates in excess of 100 Gbit/s. This approach demonstrates the capabilities of ultrafast all-optical WCs to achieve the required functionality and minimize power inefficient optical-electronic-optical (OEO) conversions for functional interfaces and network elements that run at high bit rates. The fiber WC has the potential to be compact and, with improvements in nonlinear optical technologies, to be integrated, thus making this a viable approach for ultrafast optical networks. However, to build a high-speed



(a)



(b)

Fig. 19. (a) BER characteristics after wavelength conversion and label rewriting. (b) BER characteristics for the labels.

network with the ultrafast fiber WC as described above, the cascability of the fiber WC has to be demonstrated. Our simulations indicate that the fiber WC is cascable for 10 hops and possibly more. In future research we plan to include experimental demonstration of the cascability of the fiber WC.

### Acknowledgments

The authors acknowledge funding for this research from the DARPA MOST Center for Multidisciplinary Optical Switching Technology (MOST), DARPA NGI, and the DARPA RFLICS Program. Funding and support were also provided by a grant from JDSU in cooperation with the University of California MICRO program. The authors thank Lars Grüner-Nielsen from OFS for the highly nonlinear fiber.

### References and Links

- [1] R. A. Barry, V. W. S. Chan, K. L. Hall, E. S. Kintzer, J. D. Moores, K. A. Rauschenbach, E. A. Swason, L. E. Adams, C. R. Doerr, S. G. Finn, H. A. Haus, E. P. Ippen, W. S. Wong, and M. Haner, "All-optical network consortium—ultrafast TDM networks," *IEEE J. Sel. Areas Commun.* **14**, 999–1013 (1996).
- [2] I. P. Kaminow, C. R. Doerr, C. Dragone, T. Koch U. Koren, A. A. M. Saleh, A. J. Kirby, C. M. Ozveren, B. Schofield, R. E. Thomas, R. A. Barry, D. M. Castagnozzi, V. W. S. Chan, B. R. Hemmenway, Jr., D. Marquis, S. A. Parikh, M. L. Stevens, E. A. Swanson, S. G. Finn, and R. G. Gallager, "A wideband all-optical WDM network," *IEEE J. Sel. Areas Commun.* **14**, 780–799 (1996).
- [3] V. W. S. Chan, K. L. Hall, E. Modiano, and K. A. Rauschenbach, "Architectures and technologies for high-speed optical data networks," *J. Lightwave Technol.* **16**, 2146–2168 (1998).
- [4] Y. Li and J. E. Rothenberg, "FBG-based widely tunable multichannel chromatic dispersion compensation for DWDM communications systems," in *WDM and Photonic Switching Devices for Network Applications III*, R. T. Chen and J. C. Chon, eds., Proc. SPIE 4653, 1–10 (2002).
- [5] R. S., R. G., M. B., M. Yan, C. L., and E. R.-J., "1700 km transmission at 40 Gb/s with 100 km amplifier-spacing enabled by higher-order-mode dispersion-compensation," in *27th European Conference on Optical Communications*. (IEEE, New York, 2001), pp. 282–283.
- [6] B.-E. Olsson, P. Öhlén, L. Rau, and D. J. Blumenthal, "A simple and robust 40 Gb/s wavelength converter using fiber cross-phase modulation and optical filtering," *IEEE Photonics Technol. Lett.* **12**, 846–848 (2000).
- [7] W. Wang, L. Rau, and D. J. Blumenthal, "All-optical wavelength conversion using XPM in a distributed fiber raman amplifier," in *Optical Amplifiers and Their Applications (OAA)*, Vol. 77 of OSA Trends in Optics and Photonics Series (Optical Society of America, Washington, D.C., 2002), paper OME7.
- [8] L. Rau, S. Rangarajan, D. J. Blumenthal, H.-F. Chou, Y.-J. Chiu, and J. E. Bowers, "Two-hop all-optical label swapping with variable length 80 Gb/s packets and 10 Gb/s labels using nonlinear fiber wavelength converters, unicast/multicast output and a single EAM for 80 to 10 Gb/s packet demultiplexing," in *Optical Fiber Communications Conference (OFC 2002)*, Vol. 70 of OSA Trends in Optics and Photonics Series (Optical Society of America, Washington, D.C., 2002), paper FD2–1–3.
- [9] W. Wang, H. Poulsen, L. Rau, D. J. Blumenthal, H.-F. Chou, J. E. Bowers, and L. Grüner-Nielsen, "80 Gb/s regenerative wavelength conversion using a hybrid raman/EDFA gain-enhanced XPM converter with highly-nonlinear-fiber," in *Optical Fiber Communications Conference*, Vol. 86 of OSA Trends in Optics and Photonics Series (Optical Society of America, Washington, D.C., 2003).
- [10] H.-F. Chou, Y.-J. Chiu, J. E. Bowers, W. Wang, and D. J. Blumenthal, "160 Gb/s to 10 Gb/s OTDM demultiplexing using a traveling-wave electroabsorption modulator," in *Optical Fiber Communications Conference (OFC 2003)*, Vol. 86 of OSA Trends in Optics and Photonics Series (Optical Society of America, Washington, D.C., 2003).

- [11] Y.-J. Chiu, H.-F. Chou, V. Karman, P. Abraham, and J. E. Bowers, "High extinction ratio and saturation power traveling-wave electroabsorption modulator," *IEEE Photonics Technol. Lett.* **14**, pp. 792–794 (2002).
- [12] H.-F. Chou, Y.-J. Chiu, and J. E. Bowers, "Standing-wave enhanced electroabsorption modulator for 40 GHz optical pulse generation," *IEEE Photonics Technol. Lett.* **15**, 215–217 (2003).
- [13] H.-F. Chou, Y.-J. Chiu, J. E. Bowers, L. Rau, S. Rangarajan, and D. J. Blumenthal, "Standing-wave enhanced electroabsorption modulator for 80 Gb/s to 10 Gb/s OTDM demultiplexing," in *28th European Conference on Optical Communication (ECOC 2002)* (IEEE, New York, 2002), paper 8.4.6.
- [14] J. Zhang, M. Yao, Q. Xu, H. Zhang, C. Peng, and Y. Gao, "Interferometric noise in optical time division multiplexing transmission system," *J. Lightwave Technol.* **20**, 1329–1334 (2002).
- [15] M. Nakazawa and E. Yoshida, "A 40 GHz 850 fs regeneratively FM mode-locked polarization-maintaining erbium fiber ring laser," *IEEE Photonics Technol. Lett.* **12**, 1613–1615 (2000).
- [16] B.-E. Olsson and D. J. Blumenthal, "Generation of 10 GHz pulse packets from an actively mode-locked fiber ring laser," in *Optical Fiber Communications Conference (OFC 2000)*, post-conference edition, Vol. 37 of OSA Trends in Optics and Photonics Series (Optical Society of America, Washington, D.C., 2000), pp. 175–177.
- [17] S. Bouchoule, E. Lach, G. Lemestreallan, S. Slempek, D. Mathoorasing, C. Kazmierski, and A. Ougazzaden, "High speed gain-switched laser as very simple  $4 \times 10$  Gb/s and up to  $8 \times 10$  Gb/s OTDM source," in *24th European Conference on Optical Communication (ECOC 1998)* (IEEE, New York, 1998), Vol. 1, pp. 215–216.
- [18] T. Ohno, K. Sato, R. Iga, Y. Kondo, T. Furuta, K. Yoshino, and H. Ito, "160 GHz actively modelocked semiconductor laser," *Electron. Lett.* **39**, 520–521 (2003).
- [19] B.-E. Olsson, L. Rau, and D. J. Blumenthal, "WDM to OTDM multiplexing using an ultrafast all-optical wavelength converter," *IEEE Photonics Technol. Lett.* **13**, 1005–1007 (2001).
- [20] M. R. H. Daza, H. F. Liu, M. Tsuchiya, Y. Ogawas, and T. Kamiya, "All-optical WDM-to-TDM conversion with total capacity of 33 Gb/s for WDM Network links," *J. Lightwave Technol.* **3**, 1287–1294 (1997).
- [21] M. Hayashi, H. Tanaka, K. Ohara, T. Otani, and M. Suzuki, "OTDM transmitter using WDM-TDM conversion with and electroabsorption wavelength converter," *J. Lightwave Technol.* **20**, 236–242 (2002).
- [22] S. Kawanishi, K. Okamoto, M. Ishii, O. Kamatani, H. Takara, and K. Uchiyama, "All-optical time-division-multiplexing of 100 Gbit/s signal based on four-wave mixing in a travelling-wave semiconductor laser amplifier," *Electron. Lett.* **33**, 976–977 (1997).
- [23] L. Rau, W. Wei, B.-E. Olsson, C. Yijen, C. Hsu-Feng, D. J. Blumenthal, and J. E. Bowers, "Simultaneous all-optical demultiplexing of a 40-Gb/s signal to  $4 \times 10$  Gb/s WDM channel's using an ultrafast fiber wavelength converter," *IEEE Photonics Technol. Lett.* **14**, 1725–1727 (2002).
- [24] S. Fischer, M. Duelk, M. Puleo, R. Girardi, E. Gamper, W. Vogt, W. Hunziker, E. Gini, and H. Melchior, "40-Gb/s OTDM to  $4 \times 10$  Gb/s WDM conversion in monolithic InP Mach-Zehnder interferometer module," *IEEE Photon. Technol. Lett.* **11**, 1262–1264 (1999).
- [25] K. Uchiyama and T. Morioka, "All-optical time-division demultiplexing experiment with simultaneous output of all constituent channels from 100 Gbit/s OTDM signal," *Electron. Lett.* **37**, 642–643 (2001).
- [26] K. Uchiyama, S. Kawanishi, and M. Saruwatari "100-Gb/s multiple-channel output all-optical OTDM demultiplexing using multichannel four-wave mixing in a semiconductor optical amplifier," *IEEE Photonics Technol. Lett.* **10**, 890–892 (1998).
- [27] D. Philips, A. Gloag, D. G. Moodie, N. J. Doran, I. Bennion, and A. D. Ellis, "Drop and insert multiplexing with simultaneous clock recovery using an electroabsorption modulator," *IEEE Photonics Technol. Lett.* **10**, 291–293 (1998).
- [28] St. Fischer, M. Dulk, E. Gamper, W. Vogt, W. Hunziker, E. Gini, H. Melchior, A. Buxens, H. N. Poulsen, and A. T. Clausen, "All-optical regenerative OTDM add-drop multiplexing at 40 Gb/s using monolithic InP Mach-Zehnder interferometer," *IEEE Photon. Technol. Lett.* **12**, 335–337 (2000).
- [29] L. Rau, S. Rangarajan, W. Wei, and D. J. Blumenthal, "All-optical add-drop of an OTDM chan-

- nel using an ultra-fast fiber based wavelength converter,” in *Optical Fiber Communications Conference (OFC 2002)*, Vol. 70 of OSA Trends in Optics and Photonics Series (Optical Society of America, Washington, D.C., 2002), pp. 259–261.
- [30] L. Rau, B.-E. Olsson, and D. J. Blumenthal, “Wavelength multicasting using an ultra high-speed all-optical wavelength converter,” in *Optical Fiber Communications Conference (OFC 2001)*, Vol. 58 of OSA Trends in Optics and Photonics Series (Optical Society of America, Washington, D.C., 2001), pp. WDD52-1-4.
- [31] D. J. Blumenthal, P. R. Prucnal, and J. R. Sauer, “Photonic packet switches: architectures and experimental implementations” (Invited), *Proc. IEEE* **82**, 1650–1667 (1994).
- [32] D. J. Blumenthal, “Photonic packet and all-optical label switching technologies and techniques,” invited talk presented at the Optical Fiber Communication Conference, Anaheim, Calif., 19–22 March 2002.